# The Tau MeTeR composites for the generation of continuous and categorical measures of tau deposits in the brain

**Villemagne VL[1,2,3*], Doré V [1,4], Bourgeat P[4], Burnham S[5], Mulligan R[1], Laws S[6], Fripp J[4], Cummings T[3], Salvado O[4], Masters CL[3], Rowe CC[1,2]**

[1]Department of Molecular Imaging & Therapy, Austin Health, Melbourne, Australia

[2]Department of Medicine, Austin Health, Melbourne, VIC, Australia

[3]The Florey Institute of Neuroscience and Mental Health, The University of Melbourne, Melbourne, VIC, Australia

[4]CSIRO Digital Productivity Flagship, The Australian eHealth Research Center, Brisbane, QLD, Australia

[5]eHealth, CSIRO Health and Biosecurity, Melbourne, VIC, Australia

[6]Centre of Excellence for Alzheimer's Disease Research and Care, School of Medical and Health Sciences, Edith Cowan University, Perth, WA, Australia

## Abstract

**Background:** It has been postulated that tau stereotypically spreads from the mesial temporal lobe (MTL) into neo-cortex and that tau deposition restricted to MTL might be just part of the ageing process, suggesting that both the amount and the location of these tau deposits are likely to be relevant for disease staging, prognosis, and progression. We implemented a stereospecific approach to generate both continuous and categorical measures that reflect tau spreading and deposition in order to make results from tau imaging studies clinically relevant and easy to interpret.

**Methods:** Sixty-three participants underwent tau and Aβ imaging with $^{18}$F-AV1451 and $^{18}$F-florbetapir (53-HC and 10-AD), while 27 received $^{18}$F-THK5317 and $^{18}$F-flutemetamol (22-HC and 5-AD). Three regional tau-masks were constructed: Mesial-temporal (Me) comprising entorhinal cortex, hippocampus, parahippocampus and amygdala; Temporoparietal (Te) comprising inferior temporal, fusiform, supramarginal and angular gyri, posterior cingulate/precuneus, superior and inferior parietal, and lateral occipital; and rest of neocortex (R) comprising dorsolateral and ventrolateral prefrontal, orbitofrontal, gyrus rectus, superior and middle temporal, and anterior cingulate. A neocortical tau burden was determined by averaging Te and R. Thresholds were established for each region and tracer. Z-scores were generated for each tracer to allow combination of the results. As continuous variable, a region was deemed high tau when above the 90% ile of the HC. Categorically, a study was deemed high tau when 2 of 3 regions showed high tracer retention.

**Results:** A categorical classification derived from continuous or Z-score data, yielded similar classification than obtained by applying the MeTeR scale. There were differences in the performance of the MeTeR approach between the two tracers. High cortical tau was associated with high Aβ.

**Conclusion:** We have developed a scale that accounts for the particularities of tau deposition, yielding both regional and global continuous and categorical measures of tau burden in the brain that can be applied to different tau tracers.

## Introduction

The term tauopathies categorizes neurodegenerative conditions, such as Alzheimer's disease (AD), characterized by the pathological accumulation of tau. Tau is a phosphoprotein whose major role is the stabilization of microtubules, critical for intracellular transport and cytoskeletal support.

Several selective tau tracers for positron emission tomography (PET) have been developed and evaluated in clinical studies [1-6]. For example, $^{18}$F-AV1451 (a.k.a. T807 or flortaucipir), has been widely used in the evaluation of AD and non-AD tauopathies [7,8], reporting a robust difference in tau tracer retention between cognitively normal elderly controls and AD patients [6-10]. In atypical AD presentations, $^{18}$F-AV1451 regional retention-not Aβ-amyloid as assessed by $^{11}$C-PiB-matched the clinical presentation [11].

Tau imaging studies are showing that tau tracer retention has a close relationship with markers of neuronal injury such as cortical grey matter atrophy or $^{18}$F-FDG [12,13]. Besides $^{18}$F-AV1451 [2,7], $^{18}$F-THK5317 [14] and $^{18}$F-THK5351 [6], and $^{11}$C-PBB3 [3] are also among the first-generation of selective tau PET tracers.

These tau imaging studies have confirmed the post-mortem findings that tau deposition follows a stereotypical and hierarchical distribution in the brain [15,16]. Given this sequential and hierarchical distribution of tau aggregates, we implemented and tested a stereospecific approach that can generate both continuous and categorical measures to be able to capture both tau spreading and deposition in order to make results from tau imaging studies clinically relevant and easy to interpret.

## Methods

### Subjects

Ninety participants were enrolled in the study. Participants were classified as either healthy elderly controls (HC, n=75), or meeting NINDS-ADRDA criteria for Probable AD (n=15). AD patients were recruited from Memory Disorders Clinics. Healthy control subjects were recruited by advertisement in the community. All subjects were aged over 60 years, spoke fluent English and had completed at least 7 years of education. No subjects had a history or physical or imaging findings of other neurological or psychiatric illness, current or recent drug or alcohol abuse/dependence, or any significant other disease or unstable medical condition. All participants underwent MRI consisting of a 3D T1 MPRAGE and a T2 turbospin echo sequence.

The study was approved by the Austin Health Human Research Ethics Committee. Written informed consent was obtained from all subjects prior to participation and also from the next of kin or carer for the subjects with dementia.

### Assessment of APOE genotype

APOE genotype was determined through polymerase chain reaction amplification and restrictions enzyme digestions, as previously described [17].

### Molecular imaging

Of the 90 participants, 63 participants underwent tau and Ab imaging with $^{18}$F-AV1451 and $^{18}$F-florbetapir (53 HC and 10 AD), while 27 received $^{18}$F-THK5317 and $^{18}$F-flutemetamol (22 HC and 5 AD).

All PET scans were acquired at Austin Health. Attenuation correction was performed immediately prior to imaging. For amyloid imaging studies, four 5-min frames were acquired starting either at 50 min after injection of $^{18}$F-florbetapir or 90 min after injection of $^{18}$F-flutemetamol. For tau imaging studies, four 5-min frames were acquired starting either at 80 min after injection of $^{18}$F-AV1451 or 60 min after injection of $^{18}$F-THK5317.

### Image analysis

Tau MeTeR template: By grouping individual ROI, three regional tau composite-masks were constructed (Figure 1): a. Mesial-temporal (Me) comprising entorhinal cortex, hippocampus, parahippocampus and amygdala; b.

Temporoparietal (Te) comprising inferior and middle temporal, fusiform, supramarginal and angular gyri, orbitofrontal cortex, gyrus rectus, posterior cingulate/precuneus, superior and inferior parietal, and lateral occipital; and c. Rest of neocortex (R) comprising dorsolateral and ventrolateral prefrontal, superior temporal, and anterior cingulate. A global measure of neocortical tau was calculated from the average of the Te and R composite regions.
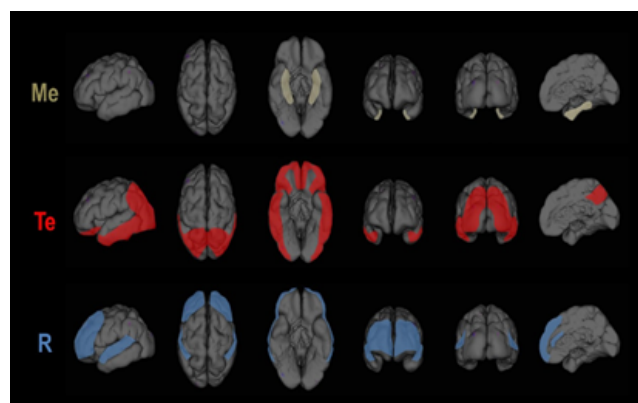


***Figure 1***. *MeTeR regional composites. Schematic representation of the MeTeR regional composites. Me (in green): mesial-temporal, comprising entorhinal cortex, hippocampus, parahippocampus and amygdala; Te (in red): temporoparietal, comprising inferior and middle temporal, fusiform, supramarginal and angular gyri, orbitofrontal cortex, gyrus rectus, posterior cingulate/precuneus, superior and inferior parietal, and lateral occipital; and R (in blue): rest of neocortex, comprising dorsolateral and ventrolateral prefrontal, superior temporal, and anterior cingulate.*

For $^{18}$F-florbetapir, Standard Uptake Value Ratios (SUVR) were generated using the whole cerebellum (SUVRWCb) as reference region, while for $^{18}$F-flutemetamol the pons (SUVRpons) was used as reference region. A 1.05 SUVRWCb and a 0.55 SUVRpons and a were selected to dichotomized the amyloid imaging studies into "high" (Aβ+) and "low" (Aβ-) for $^{18}$F-florbetapir and $^{18}$F-flutemetamol, respectively.

For both tau tracers, AV1451 and THK5317, SUVR were generated using the cerebellar cortex (SUVRCbCtx) as reference region. Global and regional SUVRCtx cut-offs for AV1451 and THK5317 were established as the respective 90%ile of the HC. Z-scores were generated using the Aβ- HC SUVRCbCtx for each tracer. A z-score threshold of 2 was selected to categorize global and regional tau as "high" (tau+) or "low" (tau-). Categorically, a tau study was deemed tau+ in the MeTeR scale when 2 of the 3 regions assessed showed high tracer retention.

### Statistical analysis

Statistical evaluations between groups were performed using ANOVA. Fisher exact test was used to compare categorical variables. Data are presented as mean ± standard deviation (SD) unless otherwise stated.

# Results

## Demographics

There were no significant differences in age between the groups. As expected, AD patients presented with worse cognition, and higher prevalence of APOE e4 carriers and high Aβ-amyloid burden in the brain. In regards to gender, while there were no significant differences between AD and HC in the AV1451 group, all 5 AD patients in the THK5317 group were female. Demographic data is presented in Table 1.

**Table 1.** Demographics. Abbreviations: HC, healthy controls; AD, Alzheimer's disease; APOE, apolipoprotein E; MMSE, Mini Mental State Examination; CDR, Clinical Dementia Rating.
*Significantly different from HC (p<0.05).*

| | AV1451 | | THK5317 | |
|---|---|---|---|---|
| | HC | AD | HC | AD |
| n | 53 | 10 | 22 | 5 |
| Age (years) | 75.0 ± 7.1 | 74.2 ± 5.4 | 75.1 ± 4.1 | 74.6 ± 4.8 |
| Gender (%Female) | 53% | 60% | 36% | 100%* |
| APOE e4 (%) | 22% | 100%* | 18% | 80%* |
| MMSE | 28.8 ± 1.1 | 24.0 ± 0.0* | 28.9 ± 1.3 | 21.2 ± 8.5* |
| CDR | 0.03 ± 0.1 | 0.67 ± 0.3* | 0.00 ± 0.0 | 1.00 ± 0.8* |
| High Ab-amyloid (%) | 27% | 100%* | 23% | 100%* |

## AV1451

Significant higher global and regional AV1451 retention was observed in AD patients when compared to controls (Figure 2, top row).
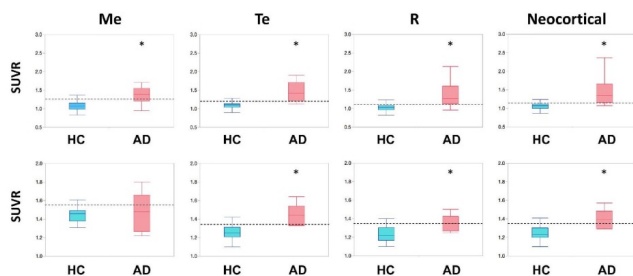


**Figure 2.** Tau burden in healthy elderly controls and Alzheimer's disease patients assessed using the MeTeR composites. Box and whiskers plots of regional (Me, Te, and R) and global (neocortical) od tau burden in healthy elderly controls (HC) and Alzheimer's disease (AD) patients as determined using two different tau tracers, AV1451 (top row) and THK5317 (bottom row). All AD patients had high Aβ-amyloid in the brain. A larger dynamic range and a higher separation between clinical classification are observed for AV1451. For both tau tracers, the temporoparietal region-Te- seems to offer the best discriminatory power between AD and controls. Dotted line denotes the respective 90% ile of the SUVR in HC, used to separate low from high tau.

The MeTeR scale classified 60% of the AD patients and 6.5% of HC as having high tau. Using the 90%ile of the HC as cut-off, 80% of the AD patients and 8.1% of HC were deemed to have high neocortical tau. When looking at regional tau burden using the classification derived from continuous variables, high tau was observed in 60% of Me, 80% of Te, and 60% of R, respectively, in AD patients and in 11.3% of Me, 11.3% of Te, and 0% of R, respectively, in HC. Considering tau status in relation to Aβ-amyloid status irrespective of clinical classification, 90% of high tau participants as classified using the MeTeR scale had high Aβ-amyloid in the brain.

## THK5317

Significant higher global and regional THK5317 retention was observed in AD patients when compared to controls (Figure 2, bottom row). The MeTeR scale classified only 20% of the AD patients and 14% of HC as having high tau. Using the 90% ile of the HC as cut-off, 60% of the AD patients and 4.6% of HC were deemed to have high neocortical tau. When looking at regional tau burden using the classification derived from continuous variables, high tau was observed in 20% of Me, 80% of Te, and 20% of R, respectively, in AD patients and in 9.1% of Me, 18.2% of Te, and 9.1% of R, respectively, in HC. Considering tau status in relation to Aβ-amyloid status irrespective of clinical classification, 50% of high tau participants as classified using the MeTeR scale had high Aβ-amyloid in the brain.

## Classification agreement

When comparing the categorical classification against Aβ-amyloid status for AV1541, 88.2% of HC with high Aβ-amyloid in the brain presented with low neocortical tau, 6.7% of HC with low Aβ-amyloid in the brain, presented with high neocortical tau, and only 60% of AD patients (100% Aβ+) presented with high neocortical tau. When assessing the results of THK5317, we observed that no HC with low Aβ-amyloid in the brain presented with high neocortical tau, and that 80% of HC with high Aβ-amyloid in the brain presented with low neocortical tau. As observed in the AV1451 group, only 60%

of AD patients (100% Aβ+) presented with high neocortical tau.

A global categorical classification derived from continuous or Z-score data, yielded similar classification than obtained by applying the MeTeR scale, with 6.3% (4/64) and 14.8% (4/27) discrepancy for AV1451 and THK5317, respectively. The overall agreement for global categorical classification derived from combining the Z-score data from both tracers was 92.2%. All discrepant cases were slightly above or below the respective thresholds.

## Discussion

It is critical to be able to obtain reliable and reproducible regional statements of tau deposition in the brain. We have learned from Aβ-amyloid imaging studies that the amount of Aβ-amyloid in the brain seems more relevant than its regional distribution as an early driver of cognitive impairment [18]. Conversely, neuropathological and initial tau imaging studies suggest that it is not only the amount, but essentially the topographical brain distribution of tau deposits that seems to be critical in driving cognitive decline and disease progression [7,19].

We have developed and implement a stereospecific approach to generate both continuous and categorical measures in order to capture the characteristics of tau deposition as well as tau spreading [15,16], stage tau imaging studies for research and clinical applications, as well as therapeutic trials [19]; allow the combination of results obtained with different tau tracers [20], facilitate the assessment of the relationship between Aβ-amyloid, tau and cognition [20], determine the prevalence of regional or global high tau in SNAP [21]; and investigate the potential to identify neuropathological defined subtypes of AD, namely typical, hippocampal sparing or limbic predominant [22]. The MeTeR approach, with its modularity, is also perfectly suited to categorize tau burden in the brain, either by including or excluding regions like the MTL, in the new ATN classification proposed by Jack et al. [23]. The ability to assess the MTL separately is important because tau accumulation in the MTL has been proposed as part of normal aging and recently named as primary age-related tauopathy (PART) [24-26]. As Prof Jack describes it: "Essentially everyone in the population develops PART at some point in life. Typically, this occurs prior to significant fibrillar amyloid deposition. By itself, however, PART produces none to mild clinical symptomatology" [27]. We have observed that high mesial temporal tau and high cortical Aβ-amyloid are present in cognitively unimpaired elderly individuals, suggesting that high widespread cortical Aβ-amyloid in addition to high mesial temporal tau deposition might not be enough to lead to significant cognitive impairment, requiring tau deposition in polymodal and unimodal association areas of the brain for objective cognitive impairment to be manifest [28].

We assessed the performance of a global and regional approach to classify tau imaging studies using two different tau tracers. We observed similar performances in classifying tau imaging studies from continuous or categorical variables. Another

important conclusion from this study is that the temporoparietal composite-Te-seems to be the most sensitive to detect cortical tau deposits, and might be used to classify and stage studies instead of the global averages. The major differences in performance were related to the tau tracers used. Given that any categorical classification is dependent on the threshold used, it could be possible that the thresholds selected for the THK5317 studies were too stringent, and a more liberal approach should be applied [29]. Moreover, the THK studies had about half of the number of participants that those who underwent AV1451, so misclassification of one or two subjects have a higher impact on the results. Another issue to be considered is the potential lack of selectivity and/or low specific binding of the tracer. THK5351, a tau tracer sharing the same basic chemical structure of THK5317, has been shown to bind to MAO-B [30]. Moreover, when compared to AV1451, THK5317 had a smaller dynamic range and lower contrast between areas with specific and non-specific binding (Figure 2). All these factors might have affected the assessments.

One of the major limitations of the study is the small number of AD cases. Despite that, the tau MeTeR scale seems to account for the particularities of tau deposition, yielding both continuous and categorical measures of tau imaging studies. The required studies to refine global and regional thresholds for these and novel tau tracers in a much larger population are on-going.

## Acknowledgements

## References

1. Fodero-Tavoletti MT, Okamura N, Furumoto S, et al. 18F-THK523: a novel in vivo tau imaging ligand for Alzheimer's disease. Brain. 2011;134(4):1089-100.

2. Chien DT, Bahri S, Szardenings AK, et al. Early clinical PET imaging results with the novel PHF-tau radioligand [F-18]-T807. J Alzheimers Dis. 2013;34(2):457-68.

3. Maruyama M, Shimada H, Suhara T, et al. Imaging of tau pathology in a tauopathy mouse model and in Alzheimer patients compared to normal controls. Neuron. 2013;79(6):1094-108.

4. Stephens A. Characterization of novel PET tracers for the assessment of tau pathology In Alzheimer's disease and other tauopathies in AD/PD. Vienna: Krager AG, Basel. 2017.

5. Walji AM, Hostetler ED, Selnick H, et al. Discovery of 6-(Fluoro-(18)F)-3-(1H-pyrrolo[2,3-c]pyridin-1-yl)isoquinolin-5-amine ([(18)F]-MK-6240): A Positron

Emission Tomography (PET) Imaging Agent for Quantification of Neurofibrillary Tangles (NFTs). J Med Chem. 2016;59(10):4778-89.

6. Okamura N, Furumoto S, Harada R, et al. Characterization of [18F]THK-5351: a novel PET tracer for imaging tau pathology in Alzheimer's disease. Eur J Nucl Med Mol Imaging. 2014;41(2):260.

7. Johnson KA, Schultz A, Betensky RA, et al. Tau positron emission tomographic imaging in aging and early Alzheimer disease. Ann Neurol. 2016;79(1):110-9.

8. Schöll M, Lockhart SN, Schonhaut DR, et al. PET Imaging of tau deposition in the aging human brain. Neuron. 2016;89(5):971-82.

9. Wang L, Benzinger TL, Su Y, et al. Evaluation of tau imaging in staging Alzheimer disease and revealing interactions between beta-amyloid and tauopathy. JAMA Neuro. 2016;73(9):1070-7.

10. Cho H, Choi JY, Hwang MS, et al. Tau PET in Alzheimer disease and mild cognitive impairment. Neurology. 2016;87(4):375-83.

11. Ossenkoppele R, Cohn-Sheehy BI, La Joie R, et al. Atrophy patterns in early clinical stages across distinct phenotypes of Alzheimer's disease. Hum Brain Mapp. 2015;36(11):4421-37.

12. Xia C, Makaretz SJ, Caso C, et al. Association of in vivo [18F]AV-1451 tau PET imaging results with cortical atrophy and symptoms in typical and atypical Alzheimer disease. JAMA Neurol. 2017;74(4):427-36.

13. Chiotis K, Saint-Aubert L, Rodriguez-Vieitez E, et al. Longitudinal changes of tau PET imaging in relation to hypometabolism in prodromal and Alzheimer's disease dementia. Mol Psychiatry. 2017.

14. Chiotis K, Saint-Aubert L, Savitcheva I, et al. Imaging in-vivo tau pathology in Alzheimer's disease with THK5317 PET in a multimodal paradigm. Eur J Nucl Med Mol Imaging. 2016;43(9):1686-99.

15. Braak H, Braak E. Frequency of stages of Alzheimer-related lesions in different age categories. Neurobiol Aging. 1997;18(4):351-7.

16. Delacourte A, David JP, Sergeant N, et al. The biochemical pathway of neurofibrillary degeneration in aging and Alzheimer's disease. Neurology. 1999;52(6):1158-65.

17. Hixson JE, Vernier DT. Restriction Isotyping of Human Apolipoprotein-E by Gene Amplification and Cleavage with HHAI. Journal of Lipid Research. 1990;31(3):545-48.

18. Rowe CC, Bourgeat P, Ellis KA, et al. Predicting Alzheimer disease with beta-amyloid imaging: results from the Australian imaging, biomarkers, and lifestyle study of ageing. Ann Neurol. 2013;74(6):905-13.

19. Villemagne VL, Fodero-Tavoletti MT, Masters CL, et al. Tau imaging: early progress and future directions. Lancet Neurol. 2015;14(1):114-24.

20. Villemagne VL, Doré V, Bourgeat P, et al. Abeta-amyloid and Tau Imaging in Dementia. Semin Nucl Med. 2017;47(1):75-88.

21. Burnham SC, Bourgeat P, Doré V, et al. Clinical and cognitive trajectories in cognitively healthy elderly individuals with suspected non-Alzheimer's disease pathophysiology (SNAP) or Alzheimer's disease pathology: a longitudinal study. Lancet Neurol. 2016;15(10):1044-53

22. Murray ME, Graff-Radford NR, Ross OA, et al. Neuropathologically defined subtypes of Alzheimer's disease with distinct clinical characteristics: a retrospective study. Lancet Neurol. 2011;10(9):785-96.

23. Jack CR Jr, Bennett DA, Blennow K, et al. A/T/N: An unbiased descriptive classification scheme for Alzheimer disease biomarkers. Neurology. 2016;87(5):539-47.

24. Crary JF, Trojanowski JQ, Schneider JA, et al. Primary age-related tauopathy (PART): a common pathology associated with human aging. Acta Neuropathol. 2014;128(6):755-66.

25. Jellinger KA, Alafuzoff I, Attems J, et al. PART a distinct tauopathy: different from classical sporadic Alzheimer disease. Acta Neuropathol. 2015.

26. Duyckaerts C, Braak H, Brion JP, et al. PART is part of Alzheimer disease. Acta Neuropathol. 2015;129(5):749-56.

27. Jack CR Jr. PART and SNAP. Acta Neuropathol. 2014;128(6):773-6.

28. Villemagne VL, Furumoto S, Fodero-Tavoletti MT, et al. In vivo evaluation of a novel tau imaging tracer for Alzheimer's disease. Eur J Nucl Med Mol Imaging. 2014;41(5):816-26.

29. Jagust WJ. Amyloid imaging:liberal or conservative? Let the data decide. Arch Neurol. 2011;68(11):1377-8.

30. Ng KP, Pascoal TA, Mathotaarachchi S, et al. Monoamine oxidase B inhibitor, selegiline, reduces 18F-THK5351 uptake in the human brain. Alzheimers Res Ther. 2017;9(1):25.

## [*]Correspondence to

Victor L Villemagne

Department of Molecular Imaging & Therapy

Austin Health, 145 Studley Road

Heidelberg, VIC. 3084

Australia

Telephone: +61-3-9496 3321

E-mail: victorlv@unimelb.edu.au